

Received January 25, 2019, accepted February 18, 2019, date of publication February 26, 2019, date of current version March 13, 2019.

Digital Object Identifier 10.1109/ACCESS.2019.2901828

Asymptotic Performance Analysis of Massive MIMO Relay Systems With Multi-Pair Devices Over Correlated Fading Channels

YI WANG^{1,2}, RUI ZHAO³, (Member, IEEE), YONGMING HUANG⁴, (Senior Member, IEEE),
CHUNGUO LI⁴, (Senior Member, IEEE), ZHENGYU ZHU⁵, (Member, IEEE),
DI ZHANG⁵, (Member, IEEE), ZHENG CHU⁶, (Member, IEEE),
AND WANMING HAO⁶, (Member, IEEE)

¹School of Intelligent Engineering, Zhengzhou University of Aeronautics, Zhengzhou 450046, China

²National Digital Switching System Engineering and Technological Research Center, Zhengzhou 450002, China

³Xiamen Key Laboratory of Mobile Multimedia Communications, Huaqiao University, Xiamen 361021, China

⁴School of Information Science and Engineering, Southeast University, Nanjing 210096, China

⁵School of Information Engineering, Zhengzhou University, Zhengzhou 450001, China

⁶5G Innovation Center, Institute of Communication Systems, University of Surrey, Guildford GU2 7XH, U.K.

Corresponding author: Yi Wang (yiwang@zua.edu.cn)

This work was supported in part by the National Natural Science Foundation of China under Grant 61801435, Grant 61801434, Grant 61720106003, Grant 61671144, and Grant U1833203, in part by the China Postdoctoral Science Foundation Project under Grant 2018M633733 and Grant 2018M642784, in part by the Scientific and Technological Key Project of Henan Province under Grant 182102210449, Grant 192102210246, Grant 192102310178, and Grant 172102210080, and in part by the Scientific Key Research Project of Henan Province for Colleges and Universities under Grant 19A510024.

ABSTRACT In this paper, we investigate a relay system with multi-pair single-antenna devices, where massive antenna array (also known as massive multiple-input-multiple-output (MIMO) technology) is deployed at the relay with low-complexity maximum-ratio combining/maximum-ratio transmission precoding scheme. By combining massive MIMO and relay cooperation, the performance of relay-assisted communication systems is predicted to be dramatically improved in many areas, e.g., spectral efficiency, energy efficiency, inter-user interference cancelation, and so on, by exploring the abundant spatial degree of freedom of massive MIMO. However, a large number of antennas employed at relay node inevitably leads to antenna correlation because of small antenna spacing subjected to the limited size of the relay node, which may affect the system performance and has not yet been compressively studied. Thus, we focus on analyzing the effect of antenna correlation on the asymptotic performance of system ergodic rate by using a general channel correlation model. First, by means of the deterministic equivalent technology, the analytical expression of the ergodic rate with arbitrary channel correlations is derived, which presents the quantitative relations among system parameters, i.e., the numbers of relay antennas and device-pairs, the channel spatial correlations at the relay's receiver side and the transmitter side, and the transmit powers of the source devices and the relay. By using a general scaling model for system parameters with respect to the relay antenna number, the asymptotic performance of the ergodic rate under spatially correlated channel and the corresponding scaling laws of the system parameters are obtained, which provides useful guidelines to trade off the transmit power and the ergodic rate as well as the number of the served device-pairs. It is further revealed that the influence degrees of the antenna correlations at the relay's receiver and the transmitter on the ergodic rate is nearly the same. Finally, the analytical conclusions are justified through the numerical simulations.

INDEX TERMS Massive MIMO relay, ergodic rate, asymptotic performance, scaling law, correlated fading channel.

I. INTRODUCTION

Multiple-input multiple-output (MIMO) technique means multiple antennas employed at the transceiver nodes, where

The associate editor coordinating the review of this manuscript and approving it for publication was Mubashir Husain Rehmani.

spatial multiplexing and diversity gain can be extracted to enhance system capacity and link reliability [1]. In traditional MIMO systems, only a few number of antennas is explored (e.g., maximal 8 antenna ports supported in 4G LTE standard), so the potential and abundant spatial resource is far from being developed on this point. Fortunately,

massive MIMO (also known as large-scale MIMO) technology, which is first put forward in multi-cell multi-user non-cooperative systems [2] by equipping a base station with tens or hundreds of antennas to serve many users under independent and identically distributed (i.i.d.) channel condition, has attracted great interests from both industry and academia [2], [2]–[5]. Through a series of exploratory researches, it has been found that massive MIMO has many distinct transmission features, e.g., producing sharp beams toward different intended users, focusing power in a specific direction, presenting asymptotic orthogonality among different users' channel vectors, and channel hardening, etc [2], [3]. Thus, massive MIMO has remarkable capability of increasing the spectral efficiency and energy efficiency by orders of magnitude, and perfectly eliminating the inter-user interference (IUI) with low-complexity linear precoding/detection scheme such as maximal-ratio combining (MRC), maximal-ratio transmission (MRT), and zero-forcing (ZF) [2]–[5]. In addition, massive MIMO has been comprehensively investigated in the areas of performance analysis [6]–[8], channel training [9], [10], pilot contamination suppression [11], [12]. Naturally, massive MIMO has been widely considered as one of the most emerging and powerful technologies for the fifth generation mobile communication systems (5G) [13].

As another promising technological avenue, two-hop relay cooperative communication has been intensively studied, which is shown to be capable of significantly enlarging the cellular coverage, reducing the power consumption and improving the throughput performance of the cell-edge users [14]. Furthermore, over decades of research, several practical relaying protocols, such as amplify-and-forward (AF) and decode-and-forward (DF) [15], [16]), have been developed and standardized. With rapidly growing requirement for higher throughput, multi-user MIMO relay systems have drawn more and more attention [17]–[19], where multiple antennas are employed at the relay to assist the information delivery between multiple source-destination pairs by exploring the spatial multiplexing and diversity gain as well as cooperative diversity. However, a major bottleneck in multi-user MIMO relay systems is the IUI, which may cause severe performance degradation [15]. Thus, many attention are paid to tackle the IUI. One intuitive way is to allocate orthogonal time/frequency resource blocks for each user pairs to avoid IUI [20], [21], which is obviously spectrally inefficient. Another line of work is to design effective precoder/detector or optimize power allocation to solve IUI [22], [23]. Whereas, it was shown in the previous works that both the precoder design and the optimal power allocation are achieved at the cost of extremely high complexity, which is not suitable for implementation in practice. Therefore, low-complexity and spectrally efficient schemes are more preferable to resolve the problem of IUI. Inspired by the characters of massive MIMO, that is, when massive antennas were used, simple linear precoding/detection can achieve near-perfect IUI elimination and near-optimal rate

performance, and massive MIMO is also introduced into multi-user relay systems.

A. RELATED WORKS

Recently, multi-user massive MIMO relaying systems have attracted more and more research activities in both academia and industry [24]–[34]. As stated above, the initial thought of employing massive antennas array at the relay node is to mitigate the IUI with high resource utilization and low-complexity processing [24]. Suraweera *et al.* [24] showed for the first time that by using massive antennas array and a simple transceiver at a relay (i.e., MRC/MRT transceiver or ZF transceiver) with ideal channel state information (CSI), the spectrum efficiency of a dual-hop one-way AF relay system becomes proportional to the number of relay antennas in multi-pair relaying system. After that, the work is extended to kinds of massive MIMO-enabled relaying systems, including half-duplex [25], [26] and full-duplex [27], [28] two-way relay systems, in the areas of performance analysis with imperfect CSI condition under different precoding schemes [29]–[31], training and data transmission design [28], [32], and energy efficiency optimization [33], [34].

In [25], the sum-rates with MRC/MRT and ZF relaying schemes under perfect CSI are analyzed for half-duplex massive MIMO two-way relaying communications via deterministic equivalence to show that the sum-rate can remain constant when the transmit power of each source and/or relay scales inversely proportional to the number of relay antennas. Jin *et al.* [26] considered the same system model as in [25] for MRC/MRT relaying where the number of relay antennas is assumed to be large but finite. Shortly afterwards, the power scaling law analysis is extended to the full-duplex massive MIMO relaying systems in [27] and [28]. In [29]–[31], one-way massive MIMO relay networks with channel estimation error are considered. While [29] used ZF relaying precoding and considered the CSI error existing in both source-relay and relay-destination links, [30] adopted MRC/MRT relaying scheme by investigating the CSI error only in the relay-destination link, based on which, [31] extended [30] to the scenario of CSI errors in dual-hop channels. In the aforesaid three works, the power scaling laws of the sources and relay for non-vanishing SINR are derived under the assumption of equal training power and data signal power. Lv *et al.* [33] and Nguyen *et al.* [34] investigated the energy-efficiency based resource allocation problem with respect to (w.r.t.) the relay antenna number and user-pair number as well as the transmit power at the user and relay for one-way and two-way networks, respectively.

B. MOTIVATIONS AND MAIN CONTRIBUTIONS

It is notable that the majority of the existing works on multi-pair massive MIMO relay systems usually assumed the i.i.d. channel conditions. In other words, the spatial correlation among the antennas at the relay is ignored. However, when large number of antennas are equipped at the relay,

the antenna spacing is very short due to the limited size of relay node together with the non-sufficient scattering environment, which will result in channel spatial correlation with a great probability. The effect of channel spatial correlation on the asymptotic performance and scaling law have not yet been fully explored in previous works on multi-pair massive MIMO AF relay system. Although antenna correlation has been studied in traditional three node MIMO relaying systems [35]–[38], which consists of a source node, a relay node and a destination node with all nodes equipped with multiple antennas, they did not take the IUI into account and has not yet analyzed the effect of antenna correlation on the system asymptotic behaviors with increasing antenna number. Furthermore, the extension of such analysis is by no means straightforward of the multi-pair massive MIMO relaying systems in terms of the asymptotic performance of ergodic rate and the scaling law.

Inspired by the aforementioned analysis, in this paper we incorporate the general antenna correlations into massive MIMO AF relay system with multi-pair devices, where the relay adopts MRC/MRT scheme. To the best of our knowledge, the impacts of antenna correlation on the asymptotic performance for such systems are still unknown. Thus, this paper address the asymptotic performance analysis and scaling laws for the multi-pair massive MIMO relay system with antenna correlation. Overall, our main contributions lies in the following aspects.

- The practical antenna correlations at the relay transceiver is taken into account for a multi-pair massive MIMO AF relay system with MRC/MRT relay precoding scheme. An analytical expression of ergodic rate is derived with arbitrary large and finite numbers of relay antennas and a general channel correlation model by using deterministic equivalents technology developed in [7] and [39]. The derived closed-form expression provides good approximation of the ergodic rate and facilitates an explicit quantitative evaluation of the ergodic rate performance.
- Based on the analytical expression, we utilize a general scaling model for the system parameters to carry out the asymptotic performance of ergodic rate as the number of relay antennas increases. The result discovers the effect and joint interaction of extensive system parameters and presents the quantitative tradeoff among different system parameters, i.e., the relay antenna number, the transmission power at the source device and the relay, the device-pair number, and the channel correlation matrices (or coefficients). Furthermore, in our scaling-law model, the scale exponents with respect to the relay antenna number can take continuous values from 0 to 1, which is different to the most existing works [24]–[34], i.e., only a few discrete values for the scaling exponents, e.g., 0, 1, and 1/2, are allowed.
- In our analysis, it is shown that when the number of device-pairs increases at a lower-than-linear speed than that of the number of relay antennas or keeps

constant, the antenna correlations at the relay's receiver and transmitter cannot affect the system scaling laws and the limit performance of ergodic rate in comparison to the i.i.d. channel condition, which only have an impact on the increment speed of the ergodic rate. This is advantageous to *facilitate the massive antennas array implemented at the relay without strict requirement of the antenna spacing*. Moreover, when the number of device-pairs increases linearly with the number of relay antennas, the scaling law is still irrelevant of the channel correlation at the relay's transceiver, but the ergodic rate will saturate to a certain limit value, which is closely related to the channel correlations.

- In addition, the uniform linear array (ULA) configuration is considered as a special case to quantitatively analyze the effect of the channel correlation degree on the system performance.

The rest of this paper is organized as follows. In Section II, the involved multi-pairs massive MIMO AF relay system is illustrated and the corresponding ergodic rate is given as performance evaluation. Section III derives the deterministic equivalent approximations about the ergodic rate first, based on which, the performance scaling law results are elaborated. In Section IV, the numerical simulations are provided to justify the effectiveness and correctness of our proposed theoretical analysis results and the conclusion is given in Section V.

Notations: Let the boldface uppercase, lowercase letters and italic letters denote matrices, vectors and scalars, respectively. $(\cdot)^T$, $(\cdot)^H$, and $\text{tr}(\cdot)$ represent the transpose, conjugate transpose, and trace operations, respectively. $[\mathbf{A}]_{i,j}$ means the i -th row and j -th column element of matrix \mathbf{A} . $\mathbb{E}\{\cdot\}$ is the statistical expectation operation. The notation $(|\cdot|)$, $\|\cdot\|$, and $\|\cdot\|_s$ indicate the absolute value, the Frobenius norm and the spectral norm, respectively. $\mathcal{CN}(\mathbf{n}, \Phi)$ stands for the circular symmetric complex Gaussian distribution with mean \mathbf{n} and covariance Φ . \mathbf{I}_N is the $(N \times N)$ identity matrix. We also use $\xrightarrow{\text{a.s.}}$ to denote the almost sure convergence.

II. SYSTEM MODEL

As depicted in Fig. 1, we consider a massive MIMO relaying system, in which K single-antenna source devices send information to their corresponding K single-antenna destination devices with the help of an N -antenna one-way AF relay. In general, N is large with $N \gg K \geq 1$. It is assumed that no direct links are available between each device pair owing to the serious path loss. Then, the MIMO relay needs to assist the data transmission between the k -th source device (S_k for short) and the k -th destination device (D_k for short), where $k = 1, \dots, K$. Both the relay and all devices work in half-duplex mode and share the same time-frequency resource. Thus, the overall transmission will take up two slots.

In the first stage, all the source devices transmit signals to the relay simultaneously, and the $N \times 1$ -dimensional received signal at the relay can be written

$$\mathbf{y}_r = \sqrt{p_s} \mathbf{H} \mathbf{x} + \mathbf{n}_r \quad (1)$$

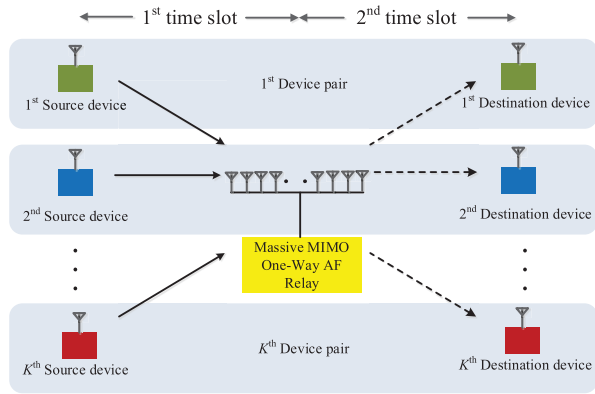


FIGURE 1. Massive MIMO one-way AF relaying system with multi-pair devices.

where $\mathbf{x} = [x_1, \dots, x_k, \dots, x_K]^T \in \mathbb{C}^{K \times 1}$ and x_k denotes the transmit signal from S_k and satisfies the power normalization, i.e., $\mathbb{E}\{|x_k|^2\} = 1$, p_s is the average transmit power at every source device, $(\mathbf{H} = [\mathbf{h}_1, \dots, \mathbf{h}_k, \dots, \mathbf{h}_K] \in \mathbb{C}^{N \times K})$ and \mathbf{h}_k means the first-hop channel vector between S_k and the relay, which can be modeled as

$$\mathbf{h}_k = \mathbf{R}_k^{1/2} \bar{\mathbf{h}}_k \tag{2}$$

where $(\mathbf{R}_k \in \mathbb{C}^{N \times N})$ is deterministic nonnegative definite spatial correlation matrix and characterizes the correlation among the receiving antennas at the relay and $\bar{\mathbf{h}}_k \sim \mathcal{CN}(0, \mathbf{I}_N)$ denotes the independent Rayleigh fast-fading channel vectors [7]. This channel model is quite general since it shows different antenna correlation of each channel vector. Furthermore, $\bar{\mathbf{h}}_k$ and $\bar{\mathbf{h}}_i$ is usually statistically independent for $k \neq i$ since different devices are located separately. $\mathbf{n}_r \sim \mathcal{CN}(0, \sigma_r^2 \mathbf{I}_N)$ is the complex additive white Gaussian noise (AWGN) vector at the relay's receiver with σ_r^2 being the noise power. Kindly note that when antenna correlation does not exist, namely i.i.d. channel condition, we only need to set $\mathbf{R}_k = \mathbf{I}_N$.

During the second phase, the received signal (\mathbf{y}_r) are converted at the relay by a linear operation, which can be expressed as $(\mathbf{y}_t = \mathbf{V}\mathbf{y}_r)$, where $\mathbf{V} \in \mathbb{C}^{N \times N}$ is a processing matrix and satisfies the total power constraint p_r at the relay, i.e.,

$$\text{tr}(\mathbb{E}\{\mathbf{y}_t \mathbf{y}_t^H\}) = \text{tr}(\mathbf{V}(p_s \mathbf{H}\mathbf{H}^H + \sigma_r^2 \mathbf{I}_N)\mathbf{V}^H) = p_r \tag{3}$$

where the expectation operation is over both data signals and noises.

To proceed, the amplified signal (\mathbf{y}_t) is disseminated to the destination devices through the relay-to-destination channel \mathbf{G}^H , where $\mathbf{G}^H = [\mathbf{g}_1, \dots, \mathbf{g}_k, \dots, \mathbf{g}_K]^H \in \mathbb{C}^{K \times N}$ and \mathbf{g}_k^H is the channel vector from the relay to D_k with $(\mathbf{g}_k^H = \bar{\mathbf{g}}_k^H \mathbf{T}_k^{1/2})$, where $\bar{\mathbf{g}}_k \sim \mathcal{CN}(0, \mathbf{I}_N)$ is the fast fading vector and \mathbf{T}_k is deterministic nonnegative definite spatial correlation matrix at the relay's transmitter side. Without loss of generality, we assume that the correlation matrices have normalized average channel gain, namely $(\text{tr}(\mathbf{R}_k) = N)$ and

$(\text{tr}(\mathbf{T}_k) = N), \forall k$. Moreover, the channel correlation matrices of both the receiver side and the transmitter side are assumed to have uniformly bounded spectral norms [7], i.e.,

$$\begin{aligned} 0 &< \limsup_{N \rightarrow \infty} \|\mathbf{R}_k\|_s < \infty \\ 0 &< \limsup_{N \rightarrow \infty} \|\mathbf{T}_k\|_s < \infty \end{aligned} \tag{4}$$

Hence, the received signal at all destination devices can be represented as

$$\mathbf{y}_d = \sqrt{p_s} \mathbf{G}^H \mathbf{V} \mathbf{H} \mathbf{x} + \sqrt{p_s} \mathbf{G}^H \mathbf{V} \mathbf{n}_r + \mathbf{n}_d \tag{5}$$

where $(\mathbf{y}_d = [y_{d,1}, \dots, y_{d,k}, \dots, y_{d,K}] \in \mathbb{C}^{K \times 1})$ with $(y_{d,k})$ being the D_k 's received signal and $(\mathbf{n}_d = [n_{d,1}, \dots, n_{d,k}, \dots, n_{d,K}] \in \mathbb{C}^{K \times 1})$ with $n_{d,k}$ being the AWGN at D_k and distributed as $(\mathcal{CN}(0, \sigma_n^2))$.

Regarding the uplink source-to-relay CSI, it can be estimated with the training sequences transmitted from the source devices. For the downlink relay-to-destination CSI, it can be obtained by means of the channel reciprocal property, which is quite common in TDD massive MIMO system. That is, the destination devices send the uplink training signals and the CSI estimation is completed at the relay as in [28] and [40]. Moreover, the global CSI can be fed back to the destination devices for further demodulation. The minimum length of the training sequences only determined by the number of antennas at the sources and destinations without any relations to the number of massive antennas at the relay. When the training sequences are sufficient long and the training power is large enough, the accuracy of channel estimation can be guaranteed to be excellent and CSI errors can be ignored. Thus, herein we assume that \mathbf{H} and \mathbf{G} are perfectly known at the relay [24], [26], [40], [41].

Based on this, one popular and widely-used AF scheme with low complexity, i.e., MRC/MRT criterion for receiving and transmitting, is adopted by the relay. Thus, the transformation matrix at the relay is given by $(\mathbf{V} = \sqrt{p_r/\theta} \mathbf{G}^H \mathbf{H})$ [24], [31], where

$$\theta = \text{tr}\left(p_s (\mathbf{H}^H \mathbf{H})^2 \mathbf{G}^H \mathbf{G} + \sigma_r^2 \mathbf{H}^H \mathbf{H} \mathbf{G}^H \mathbf{G}\right) \tag{6}$$

is a normalization factor to meet the power constraint in (3).

As a result, the received signal at D_k can be expressed in (7), as shown at the top of next page, which mainly refers to three parts [24], [31]. With the effective channel coefficient at D_k [26], i.e., $(\mathbf{g}_k^H \mathbf{G}^H \mathbf{H} \mathbf{h}_k)$, the k -th destination device will demodulate the desired signal. Furthermore, we can calculate the power of interference and noise through taking expectation w.r.t. the corresponding terms over the coherence time of the channel fading. To proceed, the expression of the signal-to-interference plus noise ratio (SINR) for D_k is given by (8), as shown at the top of next page, [24], [31].

Consequently, we can obtain the ergodic achievable rate for D_k [24], [31]

$$R_k = \mathbb{E}\left\{\frac{1}{2} \log_2(1 + \text{SINR}_{D_k})\right\}, \text{ for } k = 1, 2, \dots, K \tag{9}$$

$$y_{d,k} = \underbrace{\sqrt{\frac{p_s p_r}{\theta}} \mathbf{g}_k^H \mathbf{G} \mathbf{H}^H \mathbf{h}_k x_k}_{\text{desired signal}} + \underbrace{\sqrt{\frac{p_s p_r}{\theta}} \sum_{i=1, i \neq k}^K \mathbf{g}_k^H \mathbf{G} \mathbf{H}^H \mathbf{h}_i x_i}_{\text{inter-pair interference}} + \underbrace{\sqrt{\frac{p_r}{\theta}} \mathbf{g}_k^H \mathbf{G} \mathbf{H}^H \mathbf{n}_r + n_{d,k}}_{\text{cumulative noise}}, \quad \text{for } k = 1, 2, \dots, K \quad (7)$$

$$\text{SINR}_{D_k} = \frac{p_r p_s |\mathbf{g}_k^H \mathbf{G} \mathbf{H}^H \mathbf{h}_k|^2}{p_r p_s \sum_{i=1, i \neq k}^K |\mathbf{g}_k^H \mathbf{G} \mathbf{H}^H \mathbf{h}_i|^2 + \sigma_r^2 p_r \|\mathbf{g}_k^H \mathbf{G} \mathbf{H}^H\|^2 + \theta \sigma_n^2}, \quad \text{for } k = 1, 2, \dots, K \quad (8)$$

where the pre-log factor $\frac{1}{2}$ accounts for the time slot consumption.

Precisely, in the presence of antenna correlation, the analysis for the ergodic achievable rate is more intractable.

III. ASYMPTOTIC PERFORMANCE ANALYSIS

In this section, we deduce the performance scaling law of the massive MIMO relaying system. First, with the help of deterministic equivalent approximation technology in large-scale random matrix theory, an analytical expression of the ergodic rate is derived. Then, the general scaling law is obtained for the ergodic rate to be non-decreasing.

A. DETERMINISTIC EQUIVALENT OF ERGODIC RATE

Different from the previous works [31], [41], the closed-form expressions of the ergodic rate were derived either by using [8, Lemma 1], i.e., $(\mathbb{E} \{ \log_2 (1 + \frac{X}{Y}) \}) \approx \log_2 (1 + \frac{\mathbb{E}\{X\}}{\mathbb{E}\{Y\}})$, or by using the mean square convergence based theory [42] and Jensen’s inequality [6]. Herein, we utilize the asymptotically deterministic equivalent property, namely almost sure convergence based lemmas [7], [39], of the desired signal power term, the inter-user interference power term as well as the cumulative noise power term in the SINR expression to derive the deterministic equivalent approximation of the ergodic achievable rate.

With some tedious derivations and calculations, the deterministic equivalent analytical expression of R_k can be obtained in the following theorem, which is verified to be accurate through simulation results in Section IV.

Theorem 1: The ergodic achievable rate of the k -th destination device in the massive MIMO relay system has the following deterministic approximation

$$R_k \xrightarrow[N \rightarrow \infty]{\text{a.s.}} \bar{R}_k \triangleq \frac{1}{2} \log_2 (1 + \overline{\text{SINR}}_{D_k}) \quad (10)$$

where $\overline{\text{SINR}}_{D_k}$ is given by (11), as shown at the top of next page, with

$$\begin{cases} \varpi_{i,j} \triangleq \text{tr}(\mathbf{R}_i \mathbf{R}_j) \\ \nu_{i,j} \triangleq \text{tr}(\mathbf{T}_i \mathbf{T}_j), \end{cases} \quad i, j = 1, 2, \dots, K \quad (12)$$

Proof: Please refer to Appendix V. ■

From (10), (11) and (12), it can be seen that on the one hand, the ergodic achievable rate is highly related to the spatial correlations of both the transmitter-side antennas and

the receiver-side antennas at the relay, which are shown to be mutually coupled in the expression of $\overline{\text{SINR}}_{D_k}$. On the other hand, the expression of R_k in (10) can not be further simplified due to the non-special form of the channel spatial correlation matrices, i.e., \mathbf{R}_k and \mathbf{T}_k , unless a less general channel model or specific antenna configuration is considered, e.g., no antenna correlation case or ULA, etc..

Even though the deterministic approximation for R_k is derived in analytical expression, the result is in relation to the general second-order channel statistics, which makes the performance scaling law analysis still complicated. For analytical simplicity, we consider the scenario as in [26] and [31],¹ i.e., $T_i = T_j = T$ and $R_i = R_j = R, \forall i \neq j$, which indicates that the source/destination devices with same or similar channel spatial correlations are grouped to be served.

Then, by substituting the above conditions into (10) and after some straightforward manipulations, we have (13), as shown at the top of next page, wherein $\varpi \triangleq \text{tr} \mathbf{R}^2$ and $\nu \triangleq \text{tr} \mathbf{T}^2$. What’s more, according to the assumption in (4), it can be straightforwardly concluded that R^2 and T^2 still have uniformly bounded spectral norms. From (13), one can find that the number of device-pairs is extracted in an explicit form. Based on (13), we will study the scaling law of the ergodic achievable rate in the next subsection.

B. SCALING-LAW RESULTS AND LIMIT PERFORMANCE

In this subsection, we characterize the scaling law of the asymptotically deterministic rate \bar{R}_k in order to comprehensively analyze the effects of the system parameters on the system performance. For all system parameters, i.e., the number of device-pairs K , the transmission power of the source device p_s and the relay p_r , we adopt a general scaling model w.r.t. the number of relay antennas N . Kindly note that the involved channel spatial correlation matrices are fixed regardless of N .

¹The similar method has been made in [10], also known as JSDM scheme, which groups the users with same channel correlation features. Furthermore, You et al [11] has proved that when the number of base station antennas goes to infinity, the channel correlation matrices between the based station and different users tend to have the same channel eigen subspace spanned by the same eigenvectors with different power gain distributed at each channel eigen-directions. Thus, such grouping stratagem is easy to implement in dense user scenarios, especially for 5G typical massive machine-type communication (mMTC) applications [43].

$$\overline{\text{SINR}}_{D_k} = \frac{N^4 + \sum_{j=1, j \neq k}^K \varpi_{k,j} \nu_{k,j}}{\sum_{i=1, i \neq k}^K \left(N^2 \varpi_{k,i} + N^2 \nu_{k,i} + \sum_{j=1, j \neq k, i}^K \nu_{k,j} \varpi_{j,i} \right) + \frac{\sigma_r^2 N \left(N^2 + \sum_{j=1, k, j \neq k}^K \nu_{k,i} \right)}{P_s} + \frac{\sigma_n^2 N \sum_{i=1}^K \left(p_s N^2 + p_s \sum_{j=1, j \neq i}^K \varpi_{i,j} + \sigma_r^2 N \right)}{P_r P_s}} \quad (11)$$

$$\bar{R}_k = \frac{1}{2} \log_2 \left(1 + \frac{N^4 + (K-1) \varpi \nu}{[N^2 (\varpi + \nu) + (K-2) \varpi \nu] (K-1) + \frac{\sigma_r^2 (N^3 + (K-1) N \nu)}{P_s} + \frac{\sigma_n^2 K N (N^2 + (K-1) \varpi)}{P_r} + \frac{\sigma_n^2 \sigma_r^2 K N^2}{P_r P_s}} \right) \quad (13)$$

$$\bar{R}_k \approx \frac{1}{2} \log_2 \left(1 + \frac{N + \frac{N^{\kappa-1} \overline{\varpi \nu}}{\mu}}{\left[(\overline{\varpi + \nu}) \frac{N^\kappa}{\mu} + \overline{\varpi \nu} \frac{N^{2\kappa-1}}{\mu^2} \right] + \frac{\sigma_r^2 \left(N^\alpha + \frac{N^{\alpha+\kappa-1}}{\mu} \overline{\nu} \right)}{P_s} + \frac{\sigma_n^2 \left(N^{\beta+\kappa} + \frac{N^{\beta+2\kappa-1}}{\mu} \overline{\varpi} \right)}{\mu P_r} + \frac{\sigma_n^2 \sigma_r^2 N^{\alpha+\beta+\kappa-1}}{\mu P_r P_s}} \right) \quad (15)$$

To proceed, we give the following assumptions,

$$P_s = \frac{P_s}{N^\alpha}, \quad P_r = \frac{P_r}{N^\beta}, \quad K = \frac{N^\kappa}{\mu} \quad (14)$$

where P_s , P_r , and μ are all positive constants with P_s and P_r being regardless of N . It is worth pointing out that we should carefully set the value of μ in order to guarantee that the number of served device-pairs cannot exceed the given number of relay antennas. Therefore, $\mu \geq N^{\kappa-1}$ should be satisfied. The parameters α , β and κ depict the scales of p_s , p_r , and K w.r.t. N . By considering practical ranges of the system parameters, it is assumed that α , β , and κ all belong to $([0, 1])$. The reasons mainly lies in two-fold. First, in typical scenarios of massive MIMO, the number of devices-pairs K either grows with the number of relay antennas N or keeps constant. Thus, $\kappa \geq 0$. On the other hand, K cannot go beyond N due to the maximum available multiplexing gain is equal to the number of relay antennas N . Thus, $\kappa \leq 1$. Secondly, since the high energy efficiency is required in massive MIMO, the transmission powers at the source devices and the relay should not increase as the number of relay antennas N increases. But they can be cut down as N becomes large with a precondition that their decreasing rates are lower than the increasing rate of N . This is because that the maximum array gain used for compensating the loss of receiving energy is N . Thus $0 \leq \alpha, \beta \leq 1$.

By substituting (14) into (13) and dividing the numerator and the denominator of the SINR in (13) with N^3 , we have (15), as shown at the top of the this page, where $\left(\frac{N^\kappa}{\mu} - 1 \approx \frac{N^\kappa}{\mu} - 2 \approx \frac{N^\kappa}{\mu} \right)$ is utilized and $(\overline{\varpi} \triangleq \frac{\varpi}{N})$ and $(\overline{\nu} \triangleq \frac{\nu}{N})$ are bounded values. Therefore, the conclusion about the performance scaling laws can be obtained in the following theorem.

Theorem 2: For the multi-pair massive MIMO relaying system with MRC/MRT precoding and antenna correlations at the relay, the performance scaling exponents should satisfy the following condition in order to have a non-vanishing \bar{R}_k in (15) as $N \rightarrow \infty$

$$\max \{ \alpha, \beta + \kappa \} \leq 1, \quad 0 \leq \alpha, \beta, \kappa \leq 1 \quad (16)$$

Proof: The maximal scaling exponent w.r.t. N of each term in SINR's denominator in (15) should be less than or equal to 1. Then, the results in (16) can be obtained, which completes the proof. ■

The condition in Theorem 2 provides the available scale degrees of the source-device transmit power, the relay transmit power, and the number of the device-pairs, which is quite useful for guiding the design of the massive MIMO relay system. For example, the condition in (16) implies $\beta + \kappa \leq 1$, which indicates that to make the ergodic rate non-decreasing as the relay antenna number increasing, the scale exponent of the relay power for each source should be no less than $\frac{1}{N}$. This also puts forward a tradeoff between β and κ , i.e., the available power saving at the relay and the number of served device-pairs. With extra relay antennas, more devices can be served or less relay transmit power can be consumed for the same level of performance, but the improvements in the two aspects should satisfy the total constraint.

Precisely, when (α, β, κ) is set to be different values, \bar{R}_k in (15) will saturate to several certain levels with N going to infinity. With that in mind, we will analyze the limit performance of the ergodic rate in the following under two cases of the scales of the device-pair number, i.e., $0 \leq \kappa < 1$ and $\kappa = 1$.

1). When $0 \leq \kappa < 1$, it means that the number of device-pairs increases at a lower-than-linear speed with the relay

antenna number increasing. Then, we have the following Corollary.

Corollary 1: By assigning different scaling exponent values from (16), the ergodic rate of D_k has the following asymptotical limit performance as $N \rightarrow \infty$,

$$\bar{R}_k^\infty = \begin{cases} \frac{1}{2} \log_2(1 + c_1), & \alpha = 1, 0 \leq \beta < 1 - \kappa & (17) \\ \frac{1}{2} \log_2(1 + c_2), & \beta = 1 - \kappa, 0 \leq \alpha < 1 & (18) \\ \frac{1}{2} \log_2(1 + c_3), & \alpha = 1, \beta = 1 - \kappa & (19) \end{cases}$$

where c_1, c_2 , and c_3 are given by

$$c_1 = \frac{P_s}{\sigma_r^2}, \quad c_2 = \frac{\mu P_r}{\sigma_n^2}, \quad c_3 = \frac{1}{\frac{1}{c_1} + \frac{1}{c_2} + \frac{\sigma_n^2 \sigma_r^2}{\mu P_r P_s}} \quad (20)$$

Proof: Since μ is constant and $\bar{\omega}$ and \bar{v} are bounded values, the limit performance results in (17)-(19) can be straightforwardly deduced by keeping the dominant terms and removing the trivial terms in (15) as $N \rightarrow \infty$. This complete the proof. ■

From Corollary 1, some useful insights can be discovered as follows

- The physical meanings for (17)-(19) lies in that as the number of relay antennas becomes larger and larger, the practical transmit power at each source device, p_s , and the relay, p_r , can be continuously scaled down by $1/N^\alpha$ and $1/N^\beta$, respectively, while keeping the ergodic rate at a constant level. In the meanwhile, the number of device-pairs can increase by N^κ . From this point of view, no performance loss of the ergodic rate occurs as the actual transmit power decreases and the served number of device-pairs increases.
- It can be found that the existing work in [41], where no antenna correlations is considered at the relay, is covered as a special case in our framework. Compared with the scaling laws in [41], when $\kappa < 1$, the antenna correlations of both the relay’s receiver side and transmitter side have no impact on the system power scaling laws even on the limit values of the ergodic rate, which only depends on the predefined values P_s, P_r and μ . In other words, when a relay is equipped with a large number of antennas, we don’t have to overemphasize the sufficient antenna spacing to guarantee the independence among the antennas, which will relax the size of antenna array configuration and facilitate the deployment of the massive antenna arrays at the relay.
- Comparing (15) and (17)-(19), it is clear that the inter-pair interference term is eliminated when the number of antennas at the relay grows to infinity, since the effective relaying channels among all device pairs become pairwise orthogonal. That is, the channel asymptotic orthogonality among all device pairs is irrelevant to the spatial correlation at the relay side.
- The three scaling cases corresponds to the systems with different power capabilities at the source devices

and the relay. (17) is applicable to the systems with power limited source devices but power sufficient relay, while (18) is the opposite. For (19), it is fit for the power sufficient systems.

- From (17)-(19), one can see that the practical transmit power of the source devices and the relay can be maximally cut down by $1/N$, separately and simultaneously, at the cost of the ergodic rate performance and the number of served device-pairs. This shows the trade-off between the system power consumption, the required quality-of-service (QoS) and the subscriber capacity.

In addition to the above mentioned, when $0 \leq \alpha < 1$ and $0 \leq \beta + \kappa < 1$, it can be directly concluded from (15) that ergodic rate will keep increasing until infinity as $N \rightarrow \infty$. Because all the terms in the SINR’s denominator in (15) will tend to 0.

Unfortunately, until now we have not yet revealed the quantitative effect of the relay’s antenna correlation on the deterministic ergodic rate due to the non-special channel correlation matrices. Thus, to gain more insight, we assume the ULA configuration at the relay side, which corresponds to an exponential correlation model [44]. Then, the channel correlation matrices at the relay receiver side and the transmitter side can be represented as

$$[\mathbf{R}]_{i,j} = r^{|i-j|}, \quad [\mathbf{T}]_{i,j} = t^{|i-j|}, \quad i, j = 1, 2, \dots, N \quad (21)$$

where $0 \leq r, t \leq 1$ denote the relay’s receiver-side and transmitter-side channel correlation coefficients, respectively. The larger the antenna correlation coefficient is, the stronger the channel spatial correlation becomes. It is clear that when $r = 1$ (and/or $t = 1$), the channels at the first hop (and/or at the second hop) degenerate into i.i.d. channels.. Then, we have the following corollary.

Corollary 2: When $(\alpha, \beta, \kappa) = (0, 0, 0)$ and the high SNR region is considered, i.e., $(\frac{P_s}{\sigma_r^2} \gg 1)$ and $(\frac{P_r}{\sigma_n^2} \gg 1)$, the deterministic rate \bar{R}_k in (13) has the following approximation

$$\bar{R}_k^\infty \stackrel{N \rightarrow \infty}{\approx} \frac{1}{2} \log_2 \left(1 + \frac{N}{(K-1) \left(\frac{1+r}{1-r} + \frac{1+t}{1+t} \right)} \right) \quad (22)$$

Proof: Under the exponential correlation model, the following limit exists [45]

$$\lim_{N \rightarrow \infty} \frac{\text{tr}(\mathbf{R}^2)}{N} = \frac{1+r}{1-r}, \quad \lim_{N \rightarrow \infty} \frac{\text{tr}(\mathbf{T}^2)}{N} = \frac{1+t}{1+t} \quad (23)$$

Then, substituting (23) into (13) and ignoring the lower order terms as $N \rightarrow \infty$ yields (22). This ends the proof. ■

Obviously, the ergodic has a nearly logarithmic increase with the number of relay antennas increasing and logarithmically inversely proportional to the number of interference device pairs. What’s more, one can find that both the transmitter-side correlation and receiver-side correlation at the relay are unfavorable factors for the increment speed of the ergodic rate. Fortunately, they will not affect the trend of the rate increase. Moreover, the absolute values of

the ergodic rate will decrease in highly correlated channel, i.e., larger r and/or t .

2). When $\kappa = 1$, it indicates that the number of device-pairs increases linearly with N . Then, from (16), one can find that the power scaling exponent at the relay, β , should be equal to 0, which means that the relay power must remain constant. That is, the goal of the power saving at the relay cannot be achieved.

Specifically, with different power scaling exponent values of α , the limit performance of \bar{R}_k in (15) is summarized in the following corollary.

Corollary 3: By setting different power scaling exponent values from (16), the ergodic rate of D_k has the asymptotical limit performance shown in (24) and (25), as shown at the bottom of the this page, where ($\tilde{\omega} = \lim_{N \rightarrow \infty} \bar{\omega} < \infty$) and ($\tilde{\nu} = \lim_{N \rightarrow \infty} \bar{\nu} < \infty$).

Proof: The derivation is almost the same as the one for Corollary 1. Thus it is omitted. ■

Based on Corollary 3, we can find that the power scaling law will not be affected by the channel correlations at the relay in comparison to [41], whereas the limit values of ergodic rate is in relation to them. More precisely, the limit values of \bar{R}_k in (24) and (25) depend on μ , P_r , P_s , $\tilde{\omega}$ and $\tilde{\nu}$. However, in practical system, it means that we can still serve more devices pairs with a guaranteed QoS as the number of relay antennas increases, which is significant for the mMTC in 5G IoT networks [46], [47]. Apart from these, we can find that \bar{R}_k in (24) and (25) monotonically increases with μ , which can be proved by taking the first-order derivative of \bar{R}_k w.r.t. μ .

IV. NUMERICAL RESULTS

In this section, Monte Carlo numerical simulations are provided to verify the obtained analytical results in terms of the ergodic rate and scaling laws w.r.t. the system parameters. In each simulation, 10^4 independent channel realizations are generated and averaged to produce the numerical results. Table 1 shows the list of involved system simulation parameters with corresponding values and Table 2 specifies several scaling parameters settings. For comparison with our relaying scheme, we consider the commonly-used orthogonal channel access scheme (orthogonal scheme for short) in multi-pair MIMO relay system as benchmark [24]. More precisely, each source-destination pair occupies $\frac{1}{2K}$ channel resources for communication, which indicates that the IUI is removed completely and also means a pre-log factor $\frac{1}{2K}$. At the relay,

TABLE 1. System simulation parameters.

Parameter	Value
Noise Power: σ_r^2, σ_n^2	1W
Transmit Signal-to-Noise Ratio: $\frac{P_s}{\sigma_r^2}, \frac{P_r}{\sigma_n^2}$	10dB, 15dB
Number of Relay:	1
Number of Relay Antennas: N	[50, 500]
Number of Device-Pairs: K	[1, N]
Path-Loss Coefficient:	1
Fading Model:	Rayleigh Fading
Channel Correlation Model:	Exponential Correlation in (21)
Channel Correlation Coefficients: r, t	[0, 1]

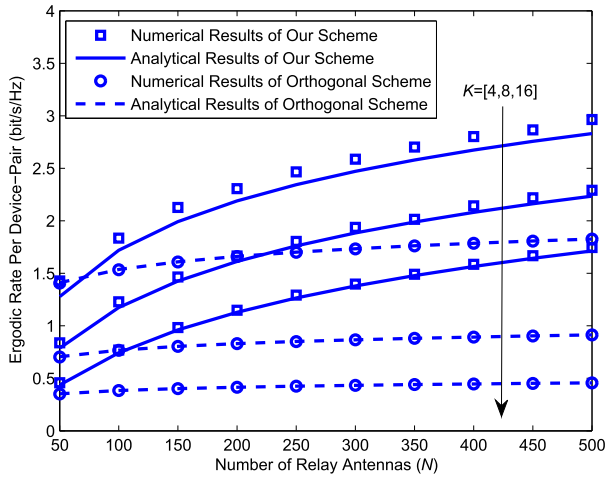
TABLE 2. Scaling parameters settings.

	α	β	κ	μ
Case 1	0	0	0	0.125
Case 2	0.5	0.5	0	0.125
Case 3	1	0.6	0	0.125
Case 4	0	1	0	0.125
Case 5	1	1	0	0.125
Case 6	1.4	1.7	0	0.125
Case 7	1	0	1	5
Case 8	1	0	1	10
Case 9	1	0	1	25
Case 10	0.3	0	1	10
Case 11	0.6	0	1	10

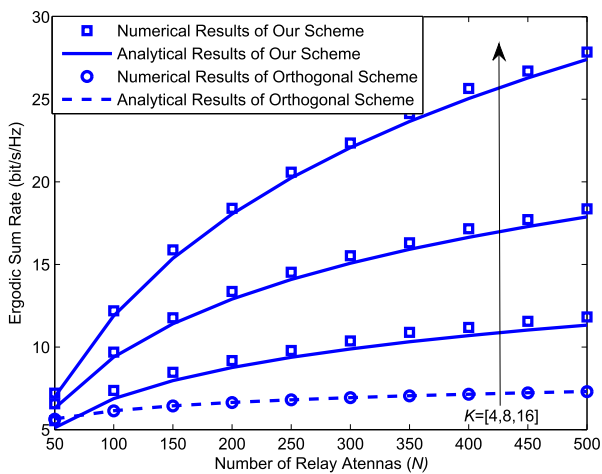
MRC/MRT is still employed for maximizing the received SINR. Obviously, the corresponding analytical expression of ergodic rate for the orthogonal scheme can be deduced from our results by setting the device-pair number $K = 1$.

Firstly, the performance of ergodic sum rate and ergodic rate per device-pair, i.e., ($R_\Sigma = \sum_{k=1}^K R_k = KR_k$) and $\bar{R} = \frac{R_\Sigma}{K} = R_k$, is given in Fig. 2 to validate the effectiveness of the proposed asymptotical deterministic equivalent expression in Theorem 1 and compare with the benchmark. It is clear that there is only tiny gap between the analytical expression and the numerical result as N increases. That is, the accuracy of the proposed analytical results is reliable. Even under the moderate number of relay antennas, the proposed analytical results can still provide good approximation. In comparison with the orthogonal scheme, it can be seen that our transmission scheme outperforms the benchmark on both the ergodic sum rate and the ergodic rate per device-pair, although no IUI exists in the orthogonal scheme. This is mainly because we benefit from simultaneously serving K device-pairs in the same time-frequency resource, which attains higher level of resources utilization. Furthermore, it is interesting to find that

$$\bar{R}_k^\infty = \begin{cases} \frac{1}{2} \log_2 \left(1 + \frac{\mu^2}{\mu(\tilde{\omega} + \tilde{\nu}) + \tilde{\omega}\tilde{\nu} + \frac{\mu^2 + \mu\tilde{\omega}}{c_2}} \right), & 0 \leq \alpha < 1, \\ \frac{1}{2} \log_2 \left(1 + \frac{\mu^2}{\mu(\tilde{\omega} + \tilde{\nu}) + \tilde{\omega}\tilde{\nu} + \frac{\mu^2 + \mu\tilde{\nu}}{c_1} + \frac{\mu^2 + \mu\tilde{\omega}}{c_2} + \frac{\mu^2}{c_1 c_2}} \right), & \alpha = 1. \end{cases} \quad (24)$$



(a)



(b)

FIGURE 2. Performance comparisons under different transmission scheme, where the transmit SNR is set as $p_s/\sigma_r^2 = p_r/\sigma_n^2 = 20\text{dB}$, $r = t = 0.5$.

the ergodic sum rate is the same for $K = [4, 8, 16]$ under the orthogonal scheme, since the same correlation conditions and path loss among the source devices and destination devices are considered here, which leads to no multi-user diversity gain. By comparing Fig. 2(a) and Fig. 2(b), one can also see that although the ergodic rate per device-pair decreases with K increasing, the sum rate grows due to the effective multi-user multiplexing gain.

Fig. 3 justifies the performance scaling laws when $0 \leq \kappa < 1$. It can be seen that for Case 1-2, R_Σ keeps increasing without a limit as N increases. While for Case 3-5, it converges to different limit values, which are given by (17)-(19), respectively. From Case 1-5, it can be found that when more power saving is preferred, i.e., larger α and/or β , the ergodic rate will be reduced accordingly, or vice versa. Specially,

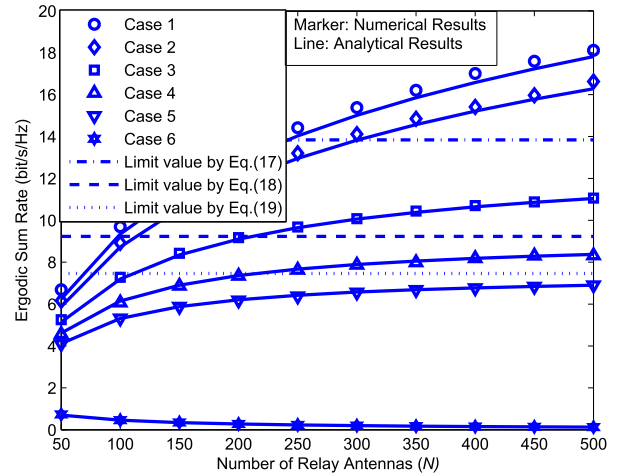


FIGURE 3. Ergodic sum rate with $0 \leq \kappa < 1$ under different (α, β, κ) , where $r = t = 0.5$.

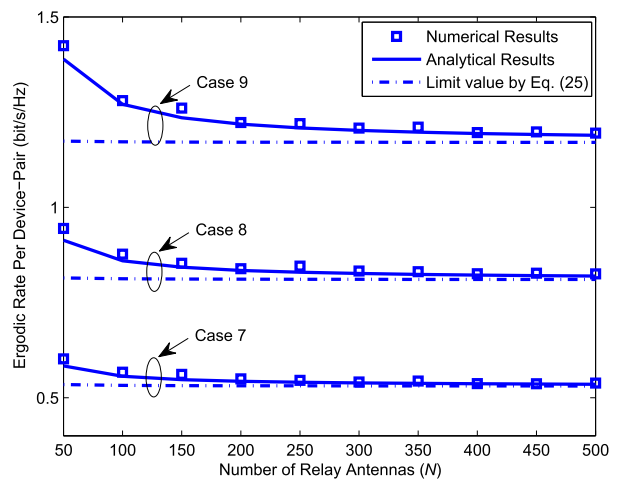


FIGURE 4. Ergodic rate per device-pair with the case $\kappa = 1$ under different μ , where $r = t = 0.5$.

the ergodic rate diminishes to zero in Case 6 as N increases, since α and β spills out of the maximal power scaling region. All the results in the figure is consistent with the scaling laws derived in Corollary 1.

Fig. 4 and Fig. 5 illustrate the performance of the ergodic rate per device-pair and ergodic sum rate as the number of user pairs K increases linearly with the number of relay antennas N , namely $\kappa = 1$, under different μ . From Fig. 4, it is seen that as $N \rightarrow \infty$, we can decrease the source device transmit power p_s by $1/N$ while the ergodic rate per device-pair is kept unchanged, which indicates that more device-pairs can be served with no loss of the current performance. Additionally, by comparing Case 7-9, it can be seen that the ergodic rate per device-pair increases with μ growing large, which is because more antennas is available for each device-pair to improve the QoS. Furthermore, in comparison with Fig. 5, although the ergodic rate per device-pair decreases with μ decreasing, the ergodic sum rate increases near-linearly over μ . This is because the multiplexing gain originated from the abundant

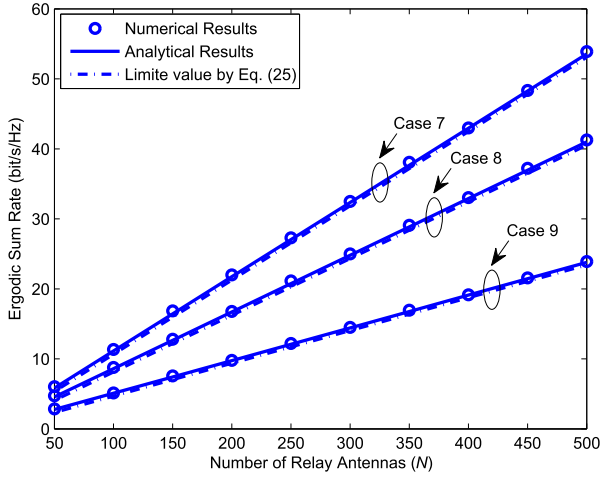


FIGURE 5. Ergodic sum rate with the case $\kappa = 1$ under different μ , where $r = t = 0.5$.

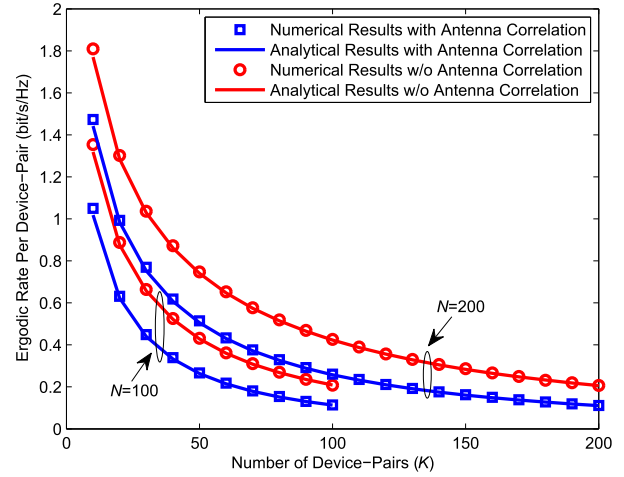


FIGURE 7. Ergodic rate per device-pair v.s. the number of device-pairs, where $(\alpha, \beta, \kappa) = (0, 0, 0)$, $r = t = 0.5$.

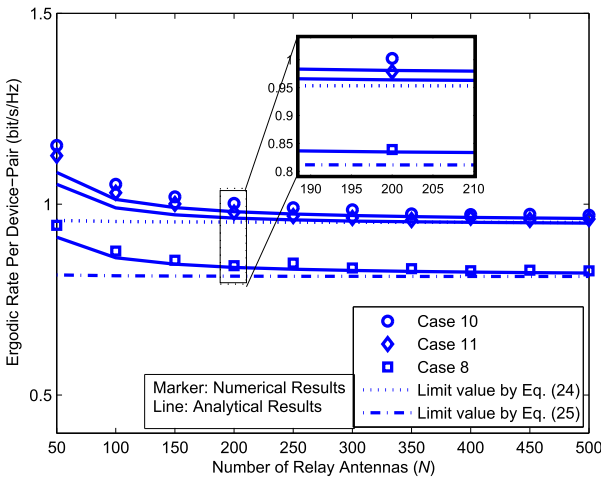


FIGURE 6. Ergodic rate per device-pair with the case $\kappa = 1$ under different scaling law.

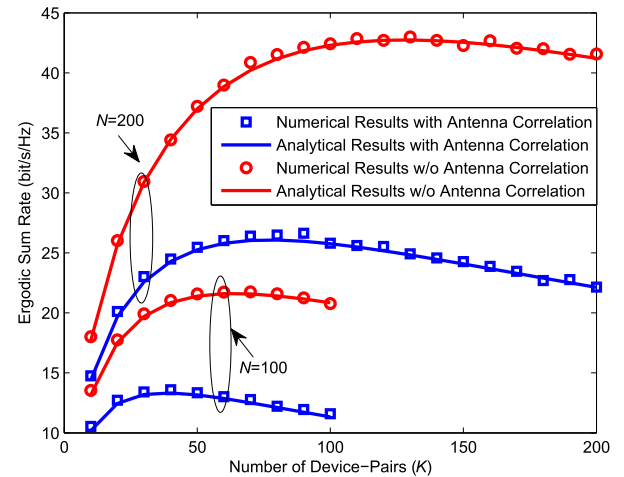


FIGURE 8. Ergodic sum rate v.s. the number of device-pairs, where $P_s/\sigma_r^2 = 10\text{dB}$, $P_r/\sigma_n^2 = 15\text{dB}$, $(\alpha, \beta, \kappa) = (0, 0, 0)$, $r = t = 0.5$.

and steadily increased DoFs of the massive antenna arrays. This further illustrates that with the continuously increasing number of antennas, we can significantly promote the network throughput by serving more and more device-pairs, which is quite suitable for the massive sensors based IoT networks with lower transmission rate requirement.

Fig. 6 shows the ergodic rate per device-pair under different power scaling exponent values with $\kappa = 1$ and $\mu = 10$. It can be seen that in Case 10-11, R_k converges to the same limit value given by (24). For Case 8, R_k tends to the limit performance given by (25), which is lower than that of Case 10-11 due to the obtained maximum power saving. Moreover, it is clear in the zoomed figure that as α becomes large, the ergodic rate decreases more seriously, which is owing to the more power saving at the source devices.

In Fig. 7, the performance of the ergodic rate per device-pair w.r.t. K is provided with and without ('w/o' for short) antenna correlation. It can be seen that for a given number

of relay antennas, R_k has a nearly logarithmic decrease with K regardless of the channel spatial correlations. Moreover, as the number of devices-pairs increases, the performance gap between the non-correlation case and the correlation case are gradually narrowed. As a comparison, the ergodic sum rate performance w.r.t. the number of device-pairs is also provided in Fig. 8. Comparing Fig. 7 and Fig. 8, it is obvious that although the performance gap is narrow for the ergodic rate per device-pair, the gap is relatively large in terms of the ergodic sum rate, which indicates that the antenna correlations intensively affects the attainable multiplexing gain.

By further observation in Fig. 8, one can find that for one thing, the ergodic sum rate no longer presents the similar monotonic increasing trend as in Fig. 5. In fact, the ergodic sum rate is first increasing and then decreasing over the number of device-pairs K . This is because when the number of relay antennas is fixed, the available multiplexing gain from numerous devices is larger than the additional inter-user interference level for small K and the ergodic sum rate decreases

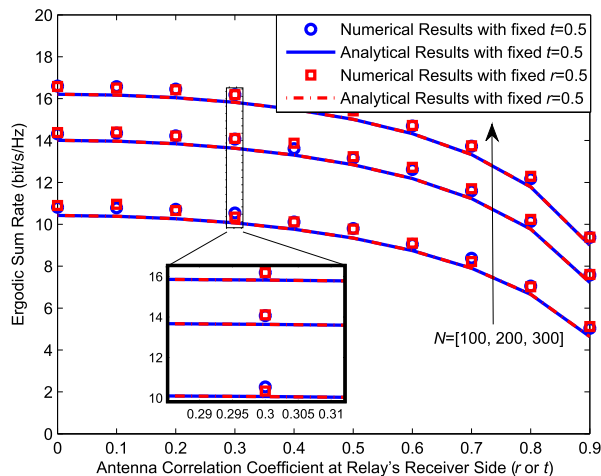


FIGURE 9. Ergodic sum rate vs. the antenna correlation at the relay, where $K = 8$ and $(\alpha, \beta, \kappa) = (0, 0, 0)$.

for large K due to the opposite reason. Hence, there exists an optimal number of served device-pairs, K^{opt} , for the ergodic sum rate maximization. Furthermore, the antenna correlation also has a negative effect on the optimal number of device-pairs. More precisely, as the channel correlation becomes strong, the supported maximum number of device-pairs will decrease. For another thing, the optimal K^{opt} increases as the number of relay antennas grows large.

In Fig. 9, the effects of the channel spatial correlations at the relay are evaluated in terms of the ergodic sum rate. Obviously, both the antenna correlation at the relay’s receiver side and the transmitter side have detrimental impacts on the ergodic rate, which lead to the performance degradation of ergodic sum rate. Especially, when the channel correlation becomes higher, namely larger r and/or t , the performance reduction speed is more quickly. From the zoomed sub-figure, it can be also found that the influence degrees of the receiver-side antenna correlation and the transmitter-side one are nearly the same, which complies with our analysis in Corollary 2.

V. CONCLUSION

In this work, we studied the performance scaling law of a multi-pair massive MIMO relay system with MRC/MRT relaying scheme. Furthermore, the spatial antenna correlation at the relay have been considered to extend the generality of the analysis. We firstly derived the asymptotical deterministic equivalents of the ergodic rate, based on which, the general scaling laws were deduced with respect to many system parameters, including the number of relay antennas, the source device transmit power, the relay transmit power as well as the number of device-pairs. Then, the asymptotically deterministic property for different scaling exponents settings are found and tradeoff between the parameters is analyzed. In our analytical results, it is revealed that the antenna correlations at the relay will not bring any effects on the scaling law but only affects the limit values of available ergodic rate.

APPENDIX A

DETERMINISTIC EQUIVALENT APPROXIMATION LEMMA

Lemma 1 ([39, Lemma 1], [7, Lemma 4]): Assume $\mathbf{Q} \in \mathbb{C}^{N \times N}$ with uniformly bounded spectral norms w.r.t. N . Consider two random vectors ($\mathbf{u} \in \mathbb{C}^{N \times 1} \sim \mathcal{CN}(\mathbf{0}, \mathbf{A})$) and ($\mathbf{v} \in \mathbb{C}^{N \times 1} \sim \mathcal{CN}(\mathbf{0}, \mathbf{B})$), which are mutually independent and independent of \mathbf{Q} . Then, we have

$$\frac{\mathbf{u}^H \mathbf{Q} \mathbf{u}}{N} - \frac{\text{tr}(\mathbf{Q} \mathbf{A})}{N} \xrightarrow[N \rightarrow \infty]{\text{a.s.}} 0 \tag{26}$$

$$\frac{\mathbf{u}^H \mathbf{Q} \mathbf{v}}{N} \xrightarrow[N \rightarrow \infty]{\text{a.s.}} 0 \tag{27}$$

$$\frac{|\mathbf{u}^H \mathbf{Q} \mathbf{v}|^2}{N^2} - \frac{\text{tr}(\mathbf{Q} \mathbf{A} \mathbf{Q} \mathbf{B})}{N^2} \xrightarrow[N \rightarrow \infty]{\text{a.s.}} 0 \tag{28}$$

APPENDIX B

PROOF OF THEOREM 1

Since $\mathbf{G} \mathbf{H}^H$ can be expressed as $\mathbf{G} \mathbf{H}^H = \sum_{j=1}^K \mathbf{g}_j \mathbf{h}_j^H$, then we substitute it into (8) and have (29)-(32), as shown at the top of next page.

It can be seen from (29)-(32) that each terms are general formulas of the sum of products of zero mean $N \times 1$ complex Gaussian vectors with different/same variance matrices, i.e., $(\mathbf{h}_l^H \mathbf{h}_m)$ and $(\mathbf{g}_l^H \mathbf{g}_m, \forall l, m = 1, 2, \dots, K)$. Then, according to Lemma 1 in Appendix A, we can obtain the deterministic equivalent approximations of $(\mathbf{h}_l^H \mathbf{h}_m)$ and $(\mathbf{g}_l^H \mathbf{g}_m)$ with $N \rightarrow \infty$

$$\frac{|\mathbf{h}_l^H \mathbf{h}_m|^n}{N^n} \xrightarrow[N \rightarrow \infty]{\text{a.s.}} \begin{cases} 0, & \text{if } l \neq m, n = 1 \\ \frac{\text{tr}(\mathbf{R}_l \mathbf{R}_m)}{N^2}, & \text{if } l \neq m, n = 2 \\ \frac{(\text{tr}(\mathbf{R}_l))^n}{N^n}, & \text{if } l = m, n \in \mathbb{Z}^+ \end{cases} \tag{33}$$

$$\frac{|\mathbf{g}_l^H \mathbf{g}_m|^n}{N^n} \xrightarrow[N \rightarrow \infty]{\text{a.s.}} \begin{cases} 0, & \text{if } l \neq m, n = 1 \\ \frac{\text{tr}(\mathbf{T}_l \mathbf{T}_m)}{N^2}, & \text{if } l \neq m, n = 2 \\ \frac{(\text{tr}(\mathbf{T}_l))^n}{N^n}, & \text{if } l = m, n \in \mathbb{Z}^+ \end{cases} \tag{34}$$

Based on (33) and (34), we can obtain the asymptotical deterministic results of the terms C_{2i-1} in (29)-(32), $i = 1, 2, \dots, 5$, as follows

$$\frac{C_1}{N^4} \xrightarrow[N \rightarrow \infty]{\text{a.s.}} \begin{cases} \frac{(\text{tr}(\mathbf{R}_k))^2 (\text{tr}(\mathbf{T}_k))^2}{N^2 N^2}, & \text{if } j = k \\ \frac{\text{tr}(\mathbf{R}_k \mathbf{R}_j)}{N^2} \frac{\text{tr}(\mathbf{T}_k \mathbf{T}_j)}{N^2}, & \text{if } j \neq k \end{cases} \tag{35}$$

$$\frac{C_3}{N^4} \xrightarrow[N \rightarrow \infty]{\text{a.s.}} \begin{cases} \frac{(\text{tr}(\mathbf{T}_k))^2 \text{tr}(\mathbf{R}_k \mathbf{R}_i)}{N^2 N^2}, & \text{if } j = k \\ \frac{\text{tr}(\mathbf{T}_k \mathbf{T}_i) (\text{tr}(\mathbf{R}_i))^2}{N^2 N^2}, & \text{if } j = i \\ \frac{\text{tr}(\mathbf{T}_k \mathbf{T}_j)}{N^2} \frac{\text{tr}(\mathbf{R}_i \mathbf{R}_j)}{N^2}, & \text{if } j \neq k, i \end{cases} \tag{36}$$

$$\frac{C_5}{N^3} \xrightarrow[N \rightarrow \infty]{\text{a.s.}} \begin{cases} \frac{(\text{tr}(\mathbf{T}_k))^2 \text{tr}(\mathbf{R}_k)}{N^2} \frac{N}{N}, & \text{if } j = k \\ \frac{\text{tr}(\mathbf{T}_k \mathbf{T}_j) \text{tr}(\mathbf{R}_j)}{N^2} \frac{N}{N}, & \text{if } j \neq k \end{cases} \tag{37}$$

$$\left| \mathbf{g}_k^H \mathbf{G} \mathbf{H}^H \mathbf{h}_k \right|^2 = \sum_{j=1}^K \sum_{l=1}^K \mathbf{g}_k^H \mathbf{g}_j \mathbf{h}_j^H \mathbf{h}_k \mathbf{h}_k^H \mathbf{h}_l \mathbf{g}_l^H \mathbf{g}_k = \sum_{j=1}^K \left(\underbrace{\left| \mathbf{g}_k^H \mathbf{g}_j \right|^2 \left| \mathbf{h}_j^H \mathbf{h}_k \right|^2}_{C_1} + \sum_{l=1, l \neq j}^K \underbrace{\mathbf{g}_k^H \mathbf{g}_j \mathbf{h}_j^H \mathbf{h}_k \mathbf{h}_k^H \mathbf{h}_l \mathbf{g}_l^H \mathbf{g}_k}_{C_2} \right) \quad (29)$$

$$\left| \mathbf{g}_k^H \mathbf{G} \mathbf{H}^H \mathbf{h}_i \right|^2 = \sum_{j=1}^K \sum_{l=1}^K \mathbf{g}_k^H \mathbf{g}_j \mathbf{h}_j^H \mathbf{h}_i \mathbf{h}_i^H \mathbf{h}_l \mathbf{g}_l^H \mathbf{g}_k = \sum_{j=1}^K \left(\underbrace{\left| \mathbf{g}_k^H \mathbf{g}_j \right|^2 \left| \mathbf{h}_j^H \mathbf{h}_i \right|^2}_{C_3} + \sum_{l=1, l \neq j}^K \underbrace{\mathbf{g}_k^H \mathbf{g}_j \mathbf{h}_j^H \mathbf{h}_i \mathbf{h}_i^H \mathbf{h}_l \mathbf{g}_l^H \mathbf{g}_k}_{C_4} \right) \quad (30)$$

$$\left\| \mathbf{g}_k^H \mathbf{G} \mathbf{H}^H \right\|^2 = \sum_{j=1}^K \sum_{l=1}^K \mathbf{g}_k^H \mathbf{g}_j \mathbf{h}_j^H \mathbf{h}_l \mathbf{g}_l^H \mathbf{g}_k = \sum_{j=1}^K \left(\underbrace{\left| \mathbf{g}_k^H \mathbf{g}_j \right|^2 \left\| \mathbf{h}_j \right\|^2}_{C_5} + \sum_{l=1, l \neq j}^K \underbrace{\mathbf{g}_k^H \mathbf{g}_j \mathbf{h}_j^H \mathbf{h}_l \mathbf{g}_l^H \mathbf{g}_k}_{C_6} \right) \quad (31)$$

$$\begin{aligned} \theta &= p_s \sum_{i=1}^K \sum_{l=1}^K \sum_{j=1}^K \mathbf{h}_i^H \mathbf{h}_j \mathbf{h}_j^H \mathbf{h}_l \mathbf{g}_l^H \mathbf{g}_i + \sigma_r^2 \sum_{i=1}^K \sum_{j=1}^K \mathbf{h}_i^H \mathbf{h}_j \mathbf{g}_j^H \mathbf{g}_i \\ &= p_s \sum_{i=1}^K \left(\sum_{j=1}^K \underbrace{\left| \mathbf{h}_i^H \mathbf{h}_j \right|^2 \left\| \mathbf{g}_i \right\|^2}_{C_7} + \sum_{l=1, l \neq i}^K \sum_{j=1}^K \underbrace{\mathbf{h}_i^H \mathbf{h}_j \mathbf{h}_j^H \mathbf{h}_l \mathbf{g}_l^H \mathbf{g}_i}_{C_8} \right) + \sigma_r^2 \sum_{i=1}^K \left(\underbrace{\left\| \mathbf{h}_i \right\|^2 \left\| \mathbf{g}_i \right\|^2}_{C_9} + \sum_{j=1, j \neq i}^K \underbrace{\mathbf{h}_i^H \mathbf{h}_j \mathbf{g}_j^H \mathbf{g}_i}_{C_{10}} \right) \end{aligned} \quad (32)$$

$$\frac{C_7}{N^3} \xrightarrow[N \rightarrow \infty]{\text{a.s.}} \begin{cases} \frac{(\text{tr}(\mathbf{R}_i))^2 \text{tr}(\mathbf{T}_i)}{N^2 N}, & \text{if } j = i \\ \frac{\text{tr}(\mathbf{R}_i \mathbf{R}_j) \text{tr}(\mathbf{T}_i)}{N^2 N}, & \text{if } j \neq i \end{cases} \quad (38)$$

$$\frac{C_9}{N^2} \xrightarrow[N \rightarrow \infty]{\text{a.s.}} \frac{\text{tr}(\mathbf{R}_i) \text{tr}(\mathbf{T}_i)}{N N} \quad (39)$$

Meanwhile, the terms $(\frac{C_2}{N^4})$, $(\frac{C_4}{N^4})$, $(\frac{C_6}{N^3})$, $(\frac{C_8}{N^3})$ and $(\frac{C_{10}}{N^2})$ will almost surely converge to 0 as $N \rightarrow \infty$.

By substituting the asymptotic deterministic approximations of C_{2i-1} into (8) and throwing away the relatively trivial terms C_{2i} ($i = 1, 2, \dots, 5$), we can obtain the corresponding asymptotic equivalents of the received SINR as $N \rightarrow \infty$

$$\text{SINR}_{D_k} \xrightarrow{\text{a.s.}} \overline{\text{SINR}}_{D_k} \quad (40)$$

where $\overline{\text{SINR}}_{D_k}$ is given in (11).

Then, on the basis of the dominated convergence and the continuous mapping theorem [7], we have the deterministic equivalent approximation of the average rate as follows

$$R_k \xrightarrow[N \rightarrow \infty]{\text{a.s.}} \frac{1}{2} \log_2 \left(1 + \overline{\text{SINR}}_{D_k} \right) \quad (41)$$

This completes the proof. ■

REFERENCES

- [1] A. Paulraj, R. Nabar, and D. Gore, *Introduction to Space-Time Wireless Communications*. Cambridge, U.K.: Cambridge Univ. Press, 2003.
- [2] T. L. Marzetta, "Noncooperative cellular wireless with unlimited numbers of base station antennas," *IEEE Trans. Wireless Commun.*, vol. 9, no. 11, pp. 3590–3600, Nov. 2010.
- [3] E. G. Larsson, O. Edfors, F. Tufvesson, and T. L. Marzetta, "Massive MIMO for next generation wireless systems," *IEEE Commun. Mag.*, vol. 52, no. 2, pp. 186–195, Feb. 2014.
- [4] E. Björnson, E. G. Larsson, and T. L. Marzetta, "Massive MIMO: Ten myths and one critical question," *IEEE Commun. Mag.*, vol. 54, no. 2, pp. 114–123, Feb. 2016.
- [5] T. L. Marzetta, E. G. Larsson, H. Yang, and H. Q. Ngo, *Fundamentals of Massive MIMO*. Cambridge, U.K.: Cambridge Univ. Press, 2016.
- [6] H. Q. Ngo, E. G. Larsson, and T. L. Marzetta, "Energy and spectral efficiency of very large multiuser MIMO systems," *IEEE Trans. Commun.*, vol. 61, no. 4, pp. 1436–1449, Apr. 2013.
- [7] J. Hoydis, S. ten Brink, and M. Debbah, "Massive MIMO in the UL/DL of cellular networks: How many antennas do we need?" *IEEE J. Sel. Areas Commun.*, vol. 31, no. 2, pp. 160–171, Feb. 2013.
- [8] Q. Zhang, S. Jin, K.-K. Wong, H. Zhu, and M. Matthaiou, "Power scaling of uplink massive MIMO systems with arbitrary-rank channel means," *IEEE J. Sel. Topics Signal Process.*, vol. 8, no. 5, pp. 966–981, Oct. 2014.
- [9] J. Choi, D. J. Love, and P. Bidigare, "Downlink training techniques for FDD massive MIMO systems: Open-loop and closed-loop training with memory," *IEEE J. Sel. Topics Signal Process.*, vol. 8, no. 5, pp. 802–814, Oct. 2014.
- [10] A. Adhikary, J. Nam, J.-Y. Ahn, and G. Caire, "Joint spatial division and multiplexing—The large-scale array regime," *IEEE Trans. Inf. Theory*, vol. 59, no. 10, pp. 6441–6463, Oct. 2013.
- [11] L. You et al., "Pilot reuse for massive MIMO transmission over spatially correlated Rayleigh fading channels," *IEEE Trans. Wireless Commun.*, vol. 14, no. 6, pp. 3352–3366, Jun. 2015.
- [12] H. Yin, L. Cottatellucci, D. Gesbert, R. R. Müller, and G. He, "Robust pilot decontamination based on joint angle and power domain discrimination," *IEEE Trans. Signal Process.*, vol. 64, no. 11, pp. 2990–3003, Jun. 2016.
- [13] C.-X. Wang et al., "Cellular architecture and key technologies for 5G wireless communication networks," *IEEE Commun. Mag.*, vol. 52, no. 2, pp. 122–130, Feb. 2014.
- [14] M. Dohler and Y. Li, *Cooperative Communications: Hardware, Channel and PHY*. Hoboken, NJ, USA: Wiley, 2010.
- [15] A. Agustin and J. Vidal, "Amplify-and-forward cooperation under interference-limited spatial reuse of the relay slot," *IEEE Trans. Wireless Commun.*, vol. 7, no. 5, pp. 1952–1962, May 2008.
- [16] Y. Zhu, P.-Y. Kam, and Y. Xin, "Differential modulation for decode-and-forward multiple relay systems," *IEEE Trans. Commun.*, vol. 58, no. 1, pp. 189–199, Jan. 2010.
- [17] S. Jin, R. McKay, C. Zhong, and K.-K. Wong, "Ergodic capacity analysis of amplify-and-forward MIMO dual-hop systems," *IEEE Trans. Inf. Theory*, vol. 56, no. 5, pp. 2204–2224, May 2010.
- [18] M. Tao and R. Wang, "Linear precoding for multi-pair two-way MIMO relay systems with max-min fairness," *IEEE Trans. Signal Process.*, vol. 60, no. 10, pp. 5361–5370, Oct. 2012.

- [19] Y. Wu, C.-K. Wen, C. Xiao, X. Gao, and R. Schober, "Linear precoding for the MIMO multiple access channel with finite alphabet inputs and statistical CSI," *IEEE Trans. Wireless Commun.*, vol. 14, no. 2, pp. 983–997, Feb. 2015.
- [20] H. Ding, J. Ge, D. B. da Costa, and Z. Jiang, "A new efficient low-complexity scheme for multi-source multi-relay cooperative networks," *IEEE Trans. Veh. Technol.*, vol. 60, no. 2, pp. 716–722, Feb. 2011.
- [21] J. Kim, D. S. Michalopoulos, and R. Schober, "Diversity analysis of multi-user multi-relay networks," *IEEE Trans. Wireless Commun.*, vol. 10, no. 7, pp. 2380–2389, Jul. 2011.
- [22] Y. Rong, X. Tang, and Y. Hua, "A unified framework for optimizing linear nonregenerative multicarrier MIMO relay communication systems," *IEEE Trans. Signal Process.*, vol. 57, no. 12, pp. 4837–4851, Dec. 2009.
- [23] F.-S. Tseng and W.-R. Wu, "Nonlinear transceiver designs in MIMO amplify-and-forward relay systems," *IEEE Trans. Veh. Technol.*, vol. 60, no. 2, pp. 528–538, Feb. 2011.
- [24] H. A. Suraweera, H. Q. Ngo, T. Q. Duong, C. Yuen, and E. G. Larsson, "Multi-pair amplify-and-forward relaying with very large antenna arrays," in *Proc. IEEE ICC*, Jun. 2013, pp. 4635–4640.
- [25] H. Cui, L. Song, and B. Jiao, "Multi-pair two-way amplify-and-forward relaying with very large number of relay antennas," *IEEE Trans. Wireless Commun.*, vol. 13, no. 5, pp. 2636–2645, May 2014.
- [26] S. Jin, X. Liang, K.-K. Wong, X. Gao, and Q. Zhu, "Ergodic rate analysis for multipair massive MIMO two-way relay networks," *IEEE Trans. Wireless Commun.*, vol. 14, no. 3, pp. 1480–1491, Mar. 2015.
- [27] H. Q. Ngo, H. A. Suraweera, M. Matthaiou, and E. G. Larsson, "Multipair full-duplex relaying with massive arrays and linear processing," *IEEE J. Sel. Areas Commun.*, vol. 32, no. 9, pp. 1721–1737, Sep. 2014.
- [28] Z. Zhang, Z. Chen, M. Shen, B. Xia, W. Xie, and Y. Zhao, "Performance analysis for training-based multipair two-way full-duplex relaying with massive antennas," *IEEE Trans. Veh. Technol.*, vol. 66, no. 7, pp. 6130–6145, Jul. 2017.
- [29] T. V. T. Le and Y. H. Kim, "Power and spectral efficiency of multi-pair massive antenna relaying systems with zero-forcing relay beamforming," *IEEE Commun. Lett.*, vol. 19, no. 2, pp. 243–246, Feb. 2015.
- [30] Y. Wang, S. Li, C. Li, Y. Huang, and L. Yang, "Ergodic rate analysis for massive MIMO relay systems with multi-pair users under imperfect CSI," in *Proc. IEEE GlobSIP*, Dec. 2015, pp. 33–37.
- [31] Q. Wang and Y. Jing, "Performance analysis and scaling law of MRC/MRT relaying with CSI error in multi-pair massive MIMO systems," *IEEE Trans. Wireless Commun.*, vol. 16, no. 9, pp. 5882–5896, Sep. 2017.
- [32] L. Pan, Y. Dai, W. Xu, and X. Dong, "Multipair massive MIMO relaying with pilot-data transmission overlay," *IEEE Trans. Wireless Commun.*, vol. 16, no. 6, pp. 3448–3460, Jun. 2017.
- [33] T. Lv, Z. Lin, P. Huang, and J. Zeng, "Optimization of the energy-efficient relay-based massive IoT network," *IEEE Internet Things J.*, vol. 5, no. 4, pp. 3043–3058, Aug. 2018.
- [34] D. D. Nguyen, Y. Liu, and Q. Chen, "On the energy efficient multi-pair two-way massive MIMO AF relaying with imperfect CSI and optimal power allocation," *IEEE Access*, vol. 6, pp. 2589–2603, 2018.
- [35] J. Wagner, B. Rankov, and A. Wittneben, "Large n analysis of amplify-and-forward MIMO relay channels with correlated Rayleigh fading," *IEEE Trans. Inf. Theory*, vol. 54, no. 12, pp. 5735–5746, Dec. 2008.
- [36] K. P. Peppas, C. K. Datsikas, N. C. Sagias, and G. S. Tombras, "Dual-hop multi-input multi-output relay systems over spatially correlated Nakagami-m fading channels," *IET Commun.*, vol. 5, no. 15, pp. 2106–2115, Oct. 2011.
- [37] R. H. Y. Louie, Y. Li, H. A. Suraweera, and B. Vucetic, "Performance analysis of beamforming in two hop amplify and forward relay networks with antenna correlation," *IEEE Trans. Wireless Commun.*, vol. 8, no. 6, pp. 3132–3141, Jun. 2009.
- [38] P. Dharmawansa, M. R. McKay, R. K. Mallik, and K. B. Letaief, "Ergodic capacity and beamforming optimality for multi-antenna relaying with statistical CSI," *IEEE Trans. Commun.*, vol. 59, no. 8, pp. 2119–2131, Aug. 2011.
- [39] K. T. Truong and R. W. Heath, "Effects of channel aging in massive MIMO systems," *J. Commun. Netw.*, vol. 15, no. 4, pp. 338–351, Aug. 2013.
- [40] M. Liu, J. Zhang, and P. Zhang, "Multipair two-way relay networks with very large antenna arrays," in *Proc. IEEE VTC Fall*, Sep. 2014, pp. 1–5.
- [41] Y. Wang et al., "Analysis over spectral efficiency and power scaling in massive MIMO dual-hop systems with multi-pair users," *IEICE Fundam. Electron., Commun. Comput. Sci.*, vol. E99-A, no. 9, pp. 1665–1673, 2016.
- [42] H. Kobayashi, B. L. Mark, and W. Turin, *Probability, Random Processes, and Statistical Analysis: Applications to Communications, Signal Processing, Queueing Theory and Mathematical Finance*. Cambridge, U.K.: Cambridge Univ. Press, 2011.
- [43] A. Osseiran et al., "Scenarios for 5G mobile and wireless communications: The vision of the METIS project," *IEEE Commun. Mag.*, vol. 52, no. 5, pp. 26–35, May 2014.
- [44] E. Björnson, J. Hoydis, M. Kountouris, and M. Debbah, "Massive MIMO systems with non-ideal hardware: Energy efficiency, estimation, and capacity limits," *IEEE Trans. Inf. Theory*, vol. 60, no. 11, pp. 7112–7139, Nov. 2014.
- [45] H. Lim, Y. Jang, and D. Yoon, "Bounds for eigenvalues of spatial correlation matrices with the exponential model in MIMO systems," *IEEE Trans. Wireless Commun.*, vol. 16, no. 2, pp. 1196–1204, Feb. 2017.
- [46] C. Bockelmann et al., "Massive machine-type communications in 5G: Physical and MAC-layer solutions," *IEEE Commun. Mag.*, vol. 54, no. 9, pp. 59–65, Sep. 2016.
- [47] J. Zou, H. Yu, W. Miao, and C. Jiang, "Packet-based preamble design for random access in massive IoT communication systems," *IEEE Access*, vol. 5, pp. 11759–11767, 2017.



YI WANG received the B.S. degree from PLA Information Engineering University, Zhengzhou, China, in 2006, and the M.S. and Ph.D. degrees from the School of Information Science and Engineering, Southeast University, China, in 2009 and 2016, respectively. Since 2016, he has been a Lecturer with the School of Electronics and Communication Engineering, which is currently reorganized as the School of Intelligent Engineering, Zhengzhou University of Aeronautics, China. From 2016 to 2019, he held a Postdoctoral Research position with the National Digital Switching System Engineering and Technological Research Center, Zhengzhou. His current research interests include massive MIMO, energy-efficient communications, cooperative communications, UAV-assisted communications, and physical-layer security. He received the Best Paper Award from the IEEE WCSP, in 2015.



RUI ZHAO (M'12) received the double bachelor's degree from the Harbin Institute of Technology, in 2003, and the M.S. and Ph.D. degrees in electrical engineering from Southeast University, China, in 2006 and 2010, respectively. After graduation, he joined the School of Information Science and Engineering, Huaqiao University, China, where he is currently an Associate Professor. From 2014 to 2015, he visited the Department of Electronic and Computer Engineering, The Hong Kong University of Science and Technology, Hong Kong, where he was a Visiting Research Scholar. His current research interests include cooperative communications, physical-layer security, and MIMO communication systems. He has published many papers in international journals such as the *IEEE TRANSACTIONS ON WIRELESS COMMUNICATIONS* and the *IEEE TRANSACTIONS ON COMMUNICATIONS*, and in conferences such as the *IEEE GLOBECOM* and the *IEEE ICC*.



YONGMING HUANG received the B.S. and M.S. degrees from Nanjing University, China, in 2000 and 2003, respectively, and the Ph.D. degree in electrical engineering from Southeast University, China, in 2007. Since 2007, he has been a Faculty Member of the School of Information Science and Engineering, Southeast University, where he is currently a Full Professor. From 2008 to 2009, he was Visiting Professor in electrical engineering with Signal Processing Lab,

Royal Institute of Technology (KTH), Stockholm, Sweden. He has published over 200 peer-reviewed papers. He holds over 40 invention patents. He has submitted over 10 technical contributions to the IEEE standards. His current research interests include MIMO wireless communications, cooperative wireless communications, and millimeter wave wireless communications. Since 2012, he has been serving as an Associate Editor for the IEEE TRANSACTIONS ON SIGNAL PROCESSING, the *EURASIP Journal on Advances in Signal Processing*, and the *EURASIP Journal on Wireless Communications and Networking*.



CHUNGUO LI received the bachelor's and Ph.D. degrees in wireless communications from Southeast University, in 2010 and 2005, respectively. In 2010, he has been a Faculty Member of Southeast University, Nanjing, where he has been an Associate Professor, since 2012. From 2012 to 2013, he held a Postdoctoral Research position at Concordia University, Montreal, Canada. In 2013, he joined the DSL laboratory supervised by Prof. J. M. Cioffi. His research interests include

the MIMO relay communications, green communications, and the next-generation of Wi-Fi. He is a Senior Member of the Chinese Institute of Electronics. He was a recipient of the Best Ph.D. Thesis Award of Southeast University, in 2010, the Excellent Foreign Postdoctoral Award of Canada, in 2012, the Science and Technology Progress Award of the National Education Ministry of China, in 2014, the Excellent Visiting Associate Professor Award at Stanford, in 2014, the Southeast University Excellent Young Professor Award, in 2015, and several conference best paper awards. He is currently the Area Editor of the *AEU-International Journal of Electronics and Communications* (Elsevier), the Associate Editor of the *Circuits, Systems, and Signal Processing*, and the Editor of the *KSII Transactions on Internet and Information Systems*. He has served in many IEEE conferences, including the IEEE 16th International Symposium on Communications and Information Technologies as the Track Chair of wireless communications, the International Conference on Communications, the International Conference on Acoustics, Speech, and Signal Processing as a TPC member. He is currently a Reviewer of many IEEE journals.



ZHENGYU ZHU received the Ph.D. degree (Hons.) in information engineering from Zhengzhou University, Zhengzhou, China, in 2017. From 2013 to 2015, he was a Visiting Student with the Wireless Communication Laboratory, Korea University, Seoul, South Korea, to conduct a collaborative research. He is currently a Lecturer with Zhengzhou University. His research interests include information theory and signal processing for wireless communications such as 5G, the Internet of Things, machine learning, UAV, massive multiple-input multiple-output wireless networks, millimeter wave communications, physical-layer security, wireless cooperative networks, convex optimization techniques, and energy harvesting communication systems.

net of Things, machine learning, UAV, massive multiple-input multiple-output wireless networks, millimeter wave communications, physical-layer security, wireless cooperative networks, convex optimization techniques, and energy harvesting communication systems.



DI ZHANG (S'13–M'17) received the Ph.D. degree from Waseda University, Tokyo, Japan, in 2017. He was a Visiting Student with the National Chung Hsing University, Taichung, Taiwan, in 2012, a Visiting Scholar with the National Key Laboratory of Alternate Electrical Power System with Renewable Energy Sources, Beijing, China, from 2015 to 2017, and a Senior Researcher with Seoul National University, Seoul, South Korea, from 2017 to 2018. He is currently

an Assistant Professor with Zhengzhou University, Zhengzhou, China. He has involved in two international projects in wireless communications and networking supported by the European FP-7, European H2020, Japanese Monbushou, and NICT. His research interests include V2X, 5G, the Internet of Things, and e-health. He serves as the Editor for the *KSII Transactions on Internet and Information Systems*, a Guest Editor of the IEEE NETWORK, the IEEE ACCESS, and *IET Intelligent Transport Systems*. He serves as a TPC member of many IEEE flagship conferences, such as the IEEE ICC, WCNC, VTC, CCNC, and Healthcom.



ZHENG CHU (M'17) received the Ph.D. degree from Newcastle University, Newcastle upon Tyne, U.K., in 2016. He was with the Faculty of Science and Technology, Middlesex University, London, U.K., from 2016 to 2017. He is currently with the 5G Innovation Center, Institute for Communication Systems, University of Surrey, Guildford, U.K. His current research interests include 5G communications, the Internet of Things, physical layer security, wireless power transfer, convex optimization techniques, and game theory.



WANMING HAO (M'18) received the Ph.D. degree from the School of Electrical and Electronic Engineering, Kyushu University, Japan, in 2018. He is currently a Research Fellow of the 5G Innovation Center, Institute of Communication Systems, University of Surrey, Guildford, U.K. His research interests include broadband wireless communication, cognitive radio, cooperative communication, massive MIMO, NOMA, HetNet, and cloud radio access networks.

...